Diabetologia (2011) 54:1169–1180
DOI 10.1007/s00125-011-2046-3

ARTICLE

Homozygous staggerer (*sg/sg*) mice display improved insulin sensitivity and enhanced glucose uptake in skeletal muscle

P. Lau · R. L. Fitzsimmons · M. A. Pearen · M. J. Watt · G. E. O. Muscat

Received: 11 October 2010 / Accepted: 3 December 2010 / Published online: 29 January 2011

Abstract
Aims/hypothesis Homozygous staggerer (*sg/sg*) mice, which have decreased and dysfunctional *Rorα* (also known as *Rora*) expression in all tissues, display a lean and dyslipidaemic phenotype. They are also resistant to (high fat) diet-induced obesity. We explored whether retinoic acid receptor-related orphan receptor (ROR) α action in skeletal muscle was involved in the regulation of glucose metabolism.
Methods We used a three-armed genomic approach, including expression profiling, ingenuity analysis and quantitative PCR validation to identify the signalling pathway(s) in skeletal muscle that are perturbed in *sg/sg* mice. Moreover, western analysis, functional insulin and glucose tolerance tests, and ex vivo glucose uptake assays were used to phenotypically characterise the impact of aberrant v-AKT murine thymoma viral oncogene homologue (AKT) signalling.
Results Homozygous and heterozygous (*sg/sg* and *sg/+*) animals exhibited decreased fasting blood glucose levels, mildly improved glucose tolerance and increased insulin sensitivity. Illumina expression profiling and bioinformatic analysis indicated the involvement of RORα in metabolic disease and phosphatidylinositol 3-kinase–AKT signalling. Quantitative PCR and western analysis validated increased AKT2 (mRNA and protein) and phosphorylation in *sg/sg* mice in the basal state. This was associated with increased expression of *Tbc1d1* and *Glut4* (also known as *Slc2a4*) mRNA and protein. Finally, in agreement with the phenotype, we observed increased (absolute) levels of AKT and phosphorylated AKT (in the basal and insulin stimulated states), and of (ex vivo) glucose uptake in skeletal muscle from *sg/sg* mice relative to wild-type littermates.
Conclusions/interpretation We propose that *Rorα* plays an important role in regulation of the AKT2 signalling cascade, which controls glucose uptake in skeletal muscle.

Keywords AKT · Glucose tolerance · Metabolism · Nuclear hormone receptor · Retinoic acid receptor-related orphan receptor alpha

Abbreviations

AKT	v-AKT murine thymoma viral oncogene homologue
EDL	Extensor digitorum longus
GAPDH	Glyceraldehyde-3-phosphate dehydrogenase
NR	Nuclear hormone receptor
pAKT	Phosphorylated AKT
PI3K	Phosphatidylinositol 3-kinase
RER	Respiratory exchange ratio
ROR	Retinoic acid receptor-related orphan receptor
ser473	Serine amino acid residue 473
TBC1D1	TBC1 domain family, member 1

Introduction

Retinoic acid receptor-related orphan receptor (ROR) alpha is a member of the nuclear hormone receptor (NR)

Electronic supplementary material The online version of this article (doi:10.1007/s00125-011-2046-3) contains supplementary material, which is available to authorised users.

P. Lau · R. L. Fitzsimmons · M. A. Pearen · G. E. O. Muscat (✉)
Obesity Research Centre, Institute for Molecular Bioscience,
The University of Queensland,
Services Rd, St Lucia,
Queensland 4072, Australia
e-mail: g.muscat@imb.uq.edu.au

M. J. Watt
Department of Physiology, Monash University,
Clayton, VIC, Australia

superfamily. NRs function as ligand-dependent DNA binding factors that translate hormonal, nutritional and pathophysiological signals into gene regulation. In the context of metabolism, NRs control lipid and glucose homeostasis in an organ- or tissue-specific manner [1–4]. It has been demonstrated that liver x receptor agonists and oxygenated sterols function as RORα/γ ligands that can suppress receptor activity [5].

Several studies on RORα [2–4, 6, 7] have revealed a role for this NR in fatty acid homeostasis [8]. Homozygous staggerer (*sg*/*sg*) mice, which have a global *Rorα* (also known as *Rora*) defect, display decreased and dysfunctional RORα (1 and 4) levels in all tissues [7, 9–11]. Moreover, *sg/sg* mice have a lean and dyslipidaemic phenotype, and are similar to *Rorα*-deficient mice (*sg* operates as a non-functional null allele) [12]. These mice display hypoalphalipoproteinaemia, decreased serum triacylglycerol and HDL-cholesterol [3], vulnerability to atherosclerosis [3], decreased fat depots and resistance to diet-induced obesity [9].

Dysfunctional NR signalling has been associated with dyslipidaemia, insulin resistance, diabetes and obesity [6, 7]. For example, the dietary lipid-dependent NRs (peroxisome proliferator-activated receptor-gamma, liver x receptor alpha etc.) in skeletal muscle regulate insulin-stimulated glucose disposal, and lipid and energy homeostasis [13–15]. Muscle is a major mass tissue that accounts for around 40% of the total body mass and energy expenditure, and is a major site of glucose disposal. Hence muscle has an important role in regulating insulin sensitivity and is increasingly recognised as an important target for combating type 2 diabetes.

Type 2 diabetes is a complex metabolic disease characterised by glucose intolerance and insulin resistance, which result in decreased insulin-mediated glucose utilisation in peripheral tissues [16]. In this context, investigation of the role of the orphan NR, RORα, in the regulation of glucose metabolism has not been completely analysed in the literature. Accordingly, we surveyed the functional role of RORα in glucose tolerance and insulin sensitivity, with particular attention to skeletal muscle.

We observed that homozygous (*sg*/*sg)* and heterozygous (*sg*/+) mice exhibited mildly improved glucose tolerance and increased insulin sensitivity. Expression profiling identified perturbations in the v-AKT murine thymoma viral oncogene homologue (AKT) signalling cascade and in genes involved in the control of glucose homeostasis. For example, we observed enhanced (absolute) levels of: (1) *Akt2* mRNA in the basal state; and (2) phosphorylated AKT (pAKT) (in the basal and insulin stimulated states); and (3) (ex vivo) glucose uptake in skeletal muscle from *sg/sg* mice relative to wild-type littermates. In summary, RORα plays an important role in regulation of the AKT signalling cascade.

Methods

Animals Heterozygous *sg*/+ mice, B6.C3(Cg)-*Rora*^{sg}/J, were obtained from Jackson laboratory (Bar Harbor, ME, USA) and maintained by backcrossing to C57BL/6 J. Feeding has been described previously [9]. Male wild-type and homozygous (*sg/sg*) mice were fed with a normal diet until 14 weeks and fasted for 6 h by transferring to a food-free holding cage with access to water. Animals were killed and tissues collected and immediately frozen in liquid nitrogen. All animal procedures were approved by The University of Queensland Animal Ethics Committee.

Glucose tolerance test Blood glucose measurements were obtained from the tail vein of 12 h fasted animals (14–16 weeks old) following glucose challenge, using a blood glucose testing system (Accu-chek Performa; Roche Diagnostics, Castle Hill, NSW, Australia) [17].

Insulin tolerance test and insulin stimulation of AKT phosphorylation Blood glucose measurements were obtained from 6 h fasted animals (14–16 weeks old) following insulin challenge, as previously described [17]. For measurement of skeletal muscle pAKT, 6 h fasted mice were administered insulin or saline as described for insulin tolerance test, killed by CO_2 asphyxiation after 10 min and quadriceps muscle excised and snap-frozen.

Microarray analysis Microarray and statistical analysis were as previously described [17] except that GeneSpring GX v7.3.1 (Agilent, Santa Clara, CA, USA) was used for analysis.

RNA extraction, cDNA synthesis and quantitative PCR Total RNA extraction, cDNA synthesis and quantitative PCR were performed as previously described [2, 9]. Primers are listed in the Electronic supplementary material (ESM) Table 1.

Protein extraction and western blot analysis Protein extraction and western analysis was performed as previously described [17] with the following modifications. The lysis buffer contained 50 mmol/l Tris (pH 8.0), 150 mmol/l NaCl, 1% (vol./vol.) Triton X-100, 1% (wt/vol.) NP40 and 0.1% (wt/vol.) SDS, and tissue was centrifuged at 2,000×*g*. Membranes were blocked with either 5% (wt/vol.) dried skimmed milk or 5% (wt/vol.) BSA (for phospho-specific antibodies). The anti-GLUT4 (number 62375; Abcam, Cambridge, MA, USA) antibody was used at 1:5,000.

2-Deoxy-D-glucose uptake assay Extensor digitorum longus (EDL) muscles were dissected from mice (3–7 months old) following cervical dislocation and 2-deoxy-D-glucose

uptake assay was performed with or without 10 nmol/l insulin stimulation (Actrapid; Nova Nordisk, Baulkham Hills, NSW, Australia) as previously described [18, 19].

Indirect calorimetry Respiratory exchange ratio (RER) was measured using a monitoring system (Oxymax Comprehensive Lab Animal System; Columbus Instruments, Columbus, OH, USA). Mice were housed individually in metabolic cages on a 12 h day–night cycle. Following an initial 14 h acclimatisation period, measurements were taken every 10 min for 24 h on normal diet (D12450B; Research Diets, New Brunswick, NJ, USA). After 24 h measurement, food was then withdrawn and measurements were taken for a further 6 h.

Statistical analysis Results were analysed by unpaired *t* test or one-way ANOVA with Bonferroni's post-hoc test, or by two-way ANOVA with Bonferroni's post hoc test; Prism 5 software (GraphPad, San Diego, CA, USA) was used.

Results

Staggerer mice present decreased fasting glucose levels, improved glucose tolerance and increased insulin sensitivity We have previously demonstrated that homozygous staggerer *(sg/sg)* mice (with decreased and dysfunctional RORα levels) display a lean phenotype. Here, we used *sg/sg* mice to elucidate the role of RORα in glucose tolerance and insulin sensitivity. We examined male wild-type and homozygous *sg/sg* mice fed a normal diet until 14 weeks and observed significantly lower blood glucose levels in homozygous *sg/sg* than in wild-type mice (n=7–11) after 6 and 12 h of fasting (Fig. 1a, b). Plasma insulin levels in the *sg/sg*, relative to wild-type mice were also decreased (but did not attain significance, p=0.08) (Fig. 1c). We further examined systemic glucose metabolism and performed intraperitoneal glucose tolerance tests. In the *sg/sg* mice, glucose clearance was mildly improved following a glucose challenge (Fig. 1d, e), with no significant differences in insulin secretion after 10 min (data not shown). The *sg/sg* mice also displayed significantly enhanced responsiveness to administration of intraperitoneal insulin, indicating enhanced whole-body insulin action compared with wild-type mice (Fig. 1f, g).

Homozygous *sg/sg* mice are characteristically lean. They display decreased adipose mass and body weight [9]. In contrast, the size:weight ratio of heterozygote (*sg/+*, haploinsufficient) mice is comparable to that of their wild-type counterparts (ESM Fig. 1a, b). The heterozygous *sg/+* mice provided a tool to investigate whether the improvement in insulin sensitivity observed in *sg/sg* mice involved differential adiposity. Therefore we investigated whether

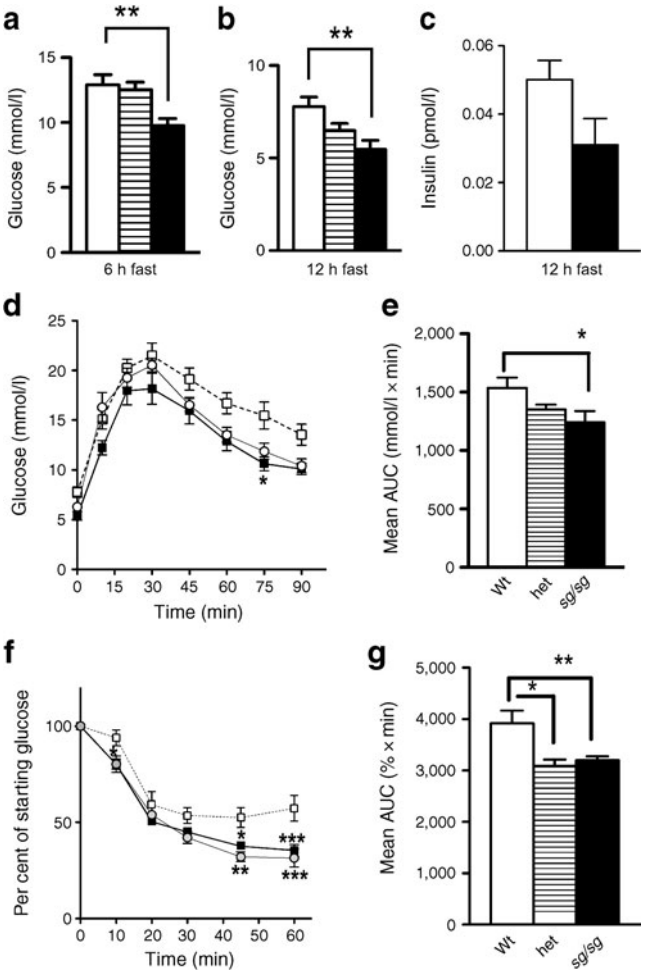

Fig. 1 **a** Starting blood glucose levels of 6 h fasted male homozygous *sg/sg* (black column), heterozygous *sg/+* (het) (striped column) and wild-type (white column) mice. These mice were used for insulin tolerance test (**f, g**); n=5–9 per group, mean±SEM; **p<0.01 by one-way ANOVA with Bonferroni's post hoc test. **b** Starting blood glucose levels of 12 h fasted mouse groups as above (**a**). These mice were used for GTT (**d, e**); n=6–11 per group, mean±SEM; **p<0.01 by one-way ANOVA with Bonferroni's post hoc test. **c** Plasma insulin concentrations of 12 h fasted male *sg/sg* wild-type littermate control mice on a regular chow diet; n=4 per group, mean±SEM. **d, e** Glucose tolerance tests. Blood glucose concentrations were measured at various times (**d**) after i.p. administration of glucose (t=0) to 12 h fasted male *sg/sg* (black squares), *sg/+* (het) (circles) and wild-type (Wt) (white squares) littermate control mice; n=6–11 per group, mean ±SEM; *p<0.05 by two-way ANOVA with Bonferroni's post hoc test. **e** Mean AUC from glucose tolerance test; mean±SEM; *p<0.05 by one-way ANOVA with Bonferroni's post hoc test. **f, g** Insulin tolerance tests. Blood glucose concentrations were measured and expressed as percentage of starting glucose (t=0) at various times (**f**) after i.p. administration of insulin (t=0) to 6 h fasted male *sg/sg* (black squares), *sg/+* (het) (circles) and wild-type littermate control (white squares) mice; n=5–9 per group, mean±SEM; *p<0.05, **p<0.01 and ***p<0.001 by two-way ANOVA with Bonferroni's post hoc test. **g** Mean AUC from insulin tolerance test; mean±SEM; *p<0.05, **p< 0.01 by one-way ANOVA with Bonferroni's post-hoc test

glucose clearance and/or insulin sensitivity were altered in *sg*/+ mice. We observed significant improvement in glucose tolerance and insulin sensitivity compared with wild-type mice (Fig. 1d–g), indicating that the increased insulin sensitivity was independent of the animal's degree of adiposity (and weight).

We also explored whether the improvement in insulin sensitivity involved a shift to (more insulin-sensitive) type I/slow fibres and/or oxidative type IIa/x fibres. Accordingly, we examined the four myosin heavy chain genes, *Myh1*, *-2*, *-4* and *-7* (in wild-type and *sg/sg* mice), which identify and classify types I, IIa, IIb and IIx fibres, respectively (ESM Fig. 2a–d). In addition, we also examined mRNA expression of the genes encoding type I and II troponin I's (*Tnni1*, *Tnni2*) (ESM Fig. 2e, f). There were no significant shifts in the mRNA expression of genes encoding any of these fibre type markers. This suggests that improved insulin sensitivity was independent of transitions in muscle fibre types.

Whole-body metabolic analysis indicated that RER in wild-type and *sg/sg* mice was similar (in the fed or dark, and fasted phases), suggesting that these lines use fats and carbohydrates for energy to a similar degree in the dark and light phases (Fig. 2a, b). The *sg/sg* mice are characteristically lean [9] and resistant to diet-induced obesity [9]. We also showed (ESM Fig. 1c, d) that on the regular chow diet

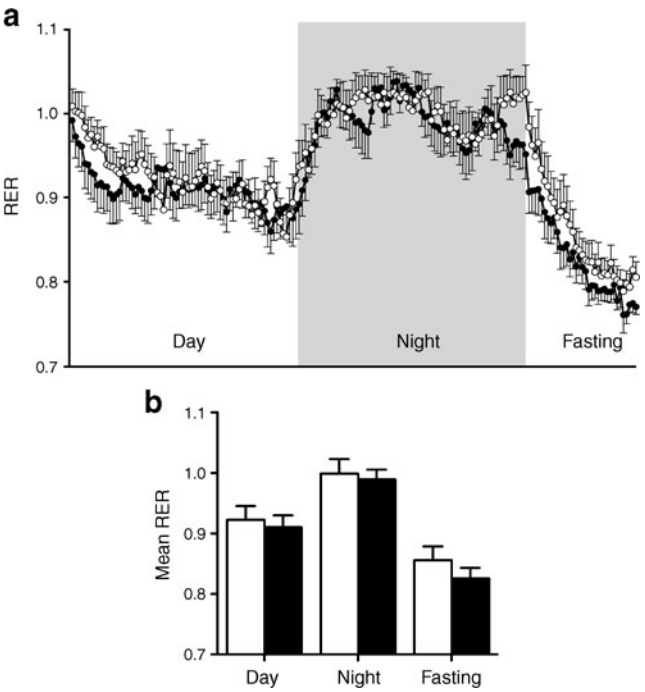

Fig. 2 CLAMS Oxymax metabolic monitoring of *sg/sg* (black circles and columns) and wild-type littermate control (white circles and columns) mice. **a** RER measurement over 12 h (day) and 12 h (night) with food and 6 h fasting. **b** Mean±SEM for RER measurement in specified phases (**a**). n=8–11 per group

the wild-type and *sg/sg* littermates ate similar quantities of food. O_2 consumption in the *sg/sg* relative to wild-type mice was significantly increased. These observations are consistent with previous reports that demonstrated a 30 to 70% higher metabolic rate (depending on temperature) and higher endogenous levels of norepinephrine in (cold-reared) *sg/sg* mice relative to control mice [20], and increased β_2*AR* (also known as *Adrb2*) mRNA expression in brown adipose tissue from *sg/sg* mice [9]. In summary, the *sg/sg* mice displayed mildly improved glucose tolerance and increased insulin sensitivity.

Expression profiling of skeletal muscle from sg/sg mice identified differential expression of genes involved in AKT signalling, and in cardiovascular and metabolic disease To probe the mechanisms underlying improved insulin sensitivity, we performed expression profiling analysis using BeadArray chips (46 K; Illumina Sentrix; Illumina, San Diego, CA, USA). Muscle (quadriceps) RNA from three male *sg/sg* mice and their wild-type littermates was utilised for analysis. Statistically significant differential up- and downregulation of annotated genes was determined on the basis of a p value cut-off of $p<0.05$ and a fold change cut-off of 1.2 as shown in Tables 1 and 2, respectively (for the complete list, see ESM Fig. 3a, b, c). All differentially expressed genes were analysed using Ingenuity Pathway Analysis (www.ingenuity.com) to examine their putative function and associated signalling pathways.

The phosphatidylinositol 3-kinase (PI3K)–AKT signalling pathway was the primary pathway to be upregulated (ESM Fig. 4c) in *sg/sg* mice. We focused on the PI3K–AKT pathway to better understand the role of RORα (and the effect of RORα deficiency) on skeletal muscle carbohydrate metabolism. Importantly, using Ingenuity Pathway Analysis, this pathway also had the highest ranking association with genes that are significantly upregulated in bead-array (Illumina) analysis. For example, the PI3K–AKT pathway had the highest ratio (4.4×10^{-2}), i.e. calculation of the number of genes in a pathway that are differentially expressed (in a significant manner) divided by the total number of known genes in that pathway. Second, it displayed a very significant p value (1.1×10^{-4}), i.e. confidence of the association between the pathway and the differentially expressed genes.

This is consistent with a phenotype displaying improved insulin sensitivity. The majority of differentially expressed genes were associated with metabolic disease, diabetes, dyslipidaemia and obesity (ESM Fig. 5).

Akt2 expression is increased in staggerer (sg/sg) mice The Ingenuity analysis identified PI3K–AKT signalling as the most significantly increased pathway. In the context of further elucidating the mechanisms involved in the control

Table 1 Upregulated annotated genes in *sg/sg* mice

Gene symbol	Gene name	Genbank ID	Fold change	*p* value
Plekhh1	Pleckstrin homology domain containing, family H (with Myth4 domain) member 1	XM_126961.4	1.97	0.002
Cidea	Cell death-inducing DNA fragmentation factor, alpha subunit-like effector a	NM_007702.1	1.69	0.039
Dnase1	Deoxyribonuclease 1	NM_010061.2	1.64	0.005
Ddit4	DNA-damage-inducible transcript 4	NM_029083.1	1.57	0.018
Synj2	Synaptojanin 2	AK038038	1.56	0.008
Tph1	Tryptophan hydroxylase 1	NM_009414.1	1.50	0.003
Cdkn1a	Cyclin-dependent kinase inhibitor 1a (p21)	NM_007669.2	1.49	0.026
Egln3	EGL nine homologue 3	AK033509	1.49	0.044
Gng2	Guanine nucleotide binding protein (G protein), gamma 2 subunit	NM_010315.2	1.48	0.000
Klk1b26	Kallikrein 1-related petidase b26	NM_010644.2	1.44	0.012
Akt2	Thymoma viral proto-oncogene 2	NM_007434.2	1.44	0.036
Tns3	Tensin-3	NM_001083587	1.44	0.027
Mt2	Metallothionein 2	NM_008630.1	1.43	0.024
Igh-1a	Immunoglobulin heavy chain 1a	XM_354704.1	1.43	0.044
Bcl2	B cell leukaemia/lymphoma 2	NM_009741.2	1.43	0.016
Chrna9	Cholinergic receptor, nicotinic, alpha polypeptide 9	XM_132045.2	1.40	0.030
Snrk	SNF related kinase	NM_133741.1	1.40	0.050
Acot11	Acyl-CoA thioesterase 11	NM_025590.4	1.39	0.033
Slc25a25	Solute carrier family 25, member 25	NM_146118.2	1.39	0.040
Syt12	Synaptotagmin 12	NM_134164.2	1.38	0.009
Foxo1	Forkhead box o1	NM_019739.2	1.37	0.040
Cdkn1a	Cyclin-dependent kinase inhibitor 1a (p21)	NM_007669.2	1.36	0.035
Tsc22d1	TSC22 domain family, member 1	NM_009366.3	1.36	0.015
Tsc22d3	TSC22 domain family, member 3	NM_010286.2	1.36	0.013
Igfbp3	Insulin-like growth factor binding protein 3	NM_008343.1	1.35	0.015
Notch4	Notch gene homologue 4 (Drosophila)	NM_010929.1	1.34	0.010
Car2	Carbonic anhydrase 2	NM_009801.3	1.34	0.005
Mt3	Metallothionein 3	NM_013603.1	1.32	0.002
Tbrg4	Transforming growth factor beta regulated gene 4	NM_134011.1	1.32	0.043
Tbc1d1	TBC1 domain family, member 1	NM_019636.1	1.31	0.004
Map3k6	Mitogen-activated protein kinase 6	NM_016693	1.31	0.046
Sox13	SRY-box containing gene 13	NM_011439.1	1.31	0.016
Shcbp1	Shc SH2-domain binding protein 1	NM_011369.1	1.30	0.033
Lmcd1	LIMand cysteine-rich domains 1	NM_144799.1	1.29	0.009
Syn2	Synapsin II	NM_013681.1	1.29	0.017
Ercc5	Excision repair cross-complementing rodent repair deficiency, complementation group 5	NM_011729.1	1.29	0.040
Syt3	Synaptotagmin 3	NM_016663.2	1.29	0.035
Car4	Carbonic anhydrase 4	NM_007607.1	1.28	0.003
Fgfr2	Fibroblast growth factor receptor 2, transcript variant 1	NM_010207.1	1.28	0.013
Dlk1	Delta-like 1 homologue (Drosophila)	NM_010052.1	1.27	0.005
Itga10	Integrin, alpha 10	XM_112192	1.27	0.026
Klk1b26	Kallikrein 1-related petidase b26	NM_010644.2	1.26	0.013
Plin3	Perilipin 3	NM_025836.3	1.26	0.004
Prom1	Prominin 1	NM_008935.1	1.26	0.002
Zbtb32	Zinc finger and BTB domain containing 32	NM_021397.2	1.26	0.041
Sh3bp2	SH3-domain binding protein 2	NM_011893	1.26	0.012
Car14	Carbonic anhydrase 14	NM_011797.1	1.25	0.001
Olfr420	Olfactory receptor 420	NM_146305.1	1.25	0.033
Fkbp5	FK506 binding protein 5	NM_010220.2	1.25	0.029
Lao1	l-amino acid oxidase 1	NM_133892.3	1.25	0.017

Table 2 Downregulated annotated genes in *sg/sg* mice

Gene symbol	Gene name	Genbank ID	Fold change	*p* value
Cpeb2	Cytoplasmic polyadenylation element binding protein 2	NM_175937	−1.79	0.007
Opn1mw	Opsin 1 (cone pigments), medium-wave-sensitive (colour blindness, deutan)	NM_008106.1	−1.70	0.026
Stab2	Stabilin 2	NM_138673.1	−1.69	0.000
Sfrp2	Secreted frizzled-related sequence protein 2	NM_009144.1	−1.65	0.025
Col7a1	Procollagen, type VII, alpha 1	NM_007738.1	−1.64	0.001
Pla2g7	Phospholipase A2, group VII (platelet-activating factor acetylhydrolase, plasma)	NM_013737.2	−1.52	0.006
Hspa1a	Heat shock protein 1a	NM_010479	−1.50	0.034
Cadm1	Cell adhesion molecule 1, transcript variant 3	NM_018770.3	−1.50	0.011
Cadm1	Cell adhesion molecule 1, transcript variant 3	NM_018770.3	−1.50	0.026
Cldn10	Claudin 10, transcript variant 2	NM_021386	−1.47	0.011
Cited4	Cbp/P300-interacting transactivator, with Glu/Asp-rich carboxy-terminal domain, 4	NM_019563	−1.45	0.046
Pogk	Pogo transposable element with KRAB domain	NM_175170	−1.45	0.007
Tiam1	T cell lymphoma invasion and metastasis 1	NM_009384.1	−1.44	0.002
Ptx3	Pentaxin related gene	NM_008987.2	−1.38	0.042
Phex	Phosphate regulating gene with homologies to endopeptidases on the X chromosome	NM_011077.1	−1.37	0.046
Ifitm6	Interferon induced transmembrane protein 6	XM_133956.3	−1.36	0.036
Gne	Glucosamine	NM_015828	−1.36	0.015
Fbn1	Fibrillin 1	AK080935	−1.34	0.020
Pon1	Paraoxonase 1	NM_011134.1	−1.34	0.020
Exph5	Exophilin 5	NM_176846.3	−1.34	0.021
Rasd2	RASD family, member 2	XM_204287.3	−1.33	0.005
Adamts1	A disintegrin-like and metalloprotease (reprolysin type) with thrombospondin type 1 motif, 1	NM_009621	−1.33	0.026
Timd4	T cell immunoglobulin and mucin domain containing 4	NM_178759.3	−1.33	0.032
Cd209d	CD209 antigen-like protein d	NM_130904.2	−1.33	0.027
Neto2	Neuropilin (NRP) and tolloid (TLL)-like 2	XM_134498	−1.33	0.050
Tekt1	Tektin 1	NM_011569.1	−1.33	0.002
Retnlg	Resistin like gamma	NM_181596.2	−1.32	0.047
Avil	Advillin	NM_009635.2	−1.32	0.003
Fgf10	Fibroblast growth factor 10	NM_008002.3	−1.31	0.036
Hist1h4b	Histone 1, H4b	NM_178193	−1.31	0.016
Jph2	Junctophilin 2	NM_021566.1	−1.30	0.042
Arhgap20	Rho Gtpase activating protein 20	NM_175535	−1.30	0.017
Fancl	Fanconi anaemia, complementation group l	NM_025923.2	−1.30	0.027
Cyhr1	Cysteine and histidine rich 1	NM_019396	−1.30	0.037
Tinag	Tubulointerstitial nephritis antigen	NM_012033.2	−1.30	0.017
Dguok	Deoxyguanosine kinase	AK003639	−1.29	0.005
Rora	Rar-related orphan receptor alpha	NM_013646.1	−1.29	0.018
Stat1	Signal transducer and activator of transcription 1	BC057690.1	−1.29	0.026
Csf-1	Colony stimulating factor 1	X05010	−1.28	0.047
Ubtf	Upstream binding transcription factor, RNA polymerase i	NM_011551	−1.28	0.020
Atxn7l2	Ataxin 7 like protein 2	NM_175183.2	−1.27	0.023
Arhgap20	Rho Gtpase activating protein 20	NM_175535	−1.27	0.038
Cd209a	CD209a antigen	NM_133238.2	−1.27	0.023
Aqp9	Aquaporin 9	NM_022026.2	−1.26	0.009
Dpysl3	Dihydropyrimidinase-like 3	NM_009468.1	−1.26	0.021
Enpp2	Ectonucleotide pyrophosphatase/phosphodiesterase 2	NM_015744	−1.26	0.000
Ache	Acetylcholinesterase	NM_009599.2	−1.26	0.016
Cul9	Cullin 9	NM_001081335	−1.26	0.039
Ube2d1	Ubiquitin-conjugating enzyme E2D 1, UBC4/5 homologue (yeast)	NM_145420.1	−1.26	0.027
Astn2	Astrotactin 2, transcript variant 1	NM_207109.1	−1.26	0.049

of glucose tolerance in the skeletal muscle of *sg/sg* mice, we used quantitative PCR to validate the differential expression of mRNAs encoding *Akt* in skeletal muscle, liver and adipose tissue of male *sg/sg* mice relative to wild-type littermates (see Fig. 3a–l).

We observed significantly increased levels of *Akt1* and *Akt2* (variant 2) mRNA, but not of *Akt3* mRNA in muscle from (fasted) *sg/sg* mice (Fig. 3a–d). Interestingly, two variants of *Akt2* have been described in the NCBI database (ncbi.nlm.nih.gov/nucleotide, accessed 17 December 2010). Variants 1 and 2 are produced by alternate promoter usage and result in exon 1 encoding different 5′ untranslated region sequences (Fig. 3m). Variant 2, but not variant 1, mRNA was increased in staggerer mice (Fig. 3b, c). Notably, no significant changes in *Akt1*, *Akt2* (variants 1 and 2) or *Akt3* mRNA expression were observed in liver or adipose tissue (Fig. 3e–i).

Levels of *Rorα* mRNA in the muscle of heterozygous staggerer mice are approximately half of those in wild-type mice (ESM Fig. 1b). To understand further the effect of *Rorα* expression on transcription of *Akt* isoforms, we analysed the expression of *Akt1*, *Akt2* variant 1 and *Akt2* variant 2 mRNAs in the heterozygote (RORα haploinsufficient mice). The expression of *Akt2* variant 2 (but

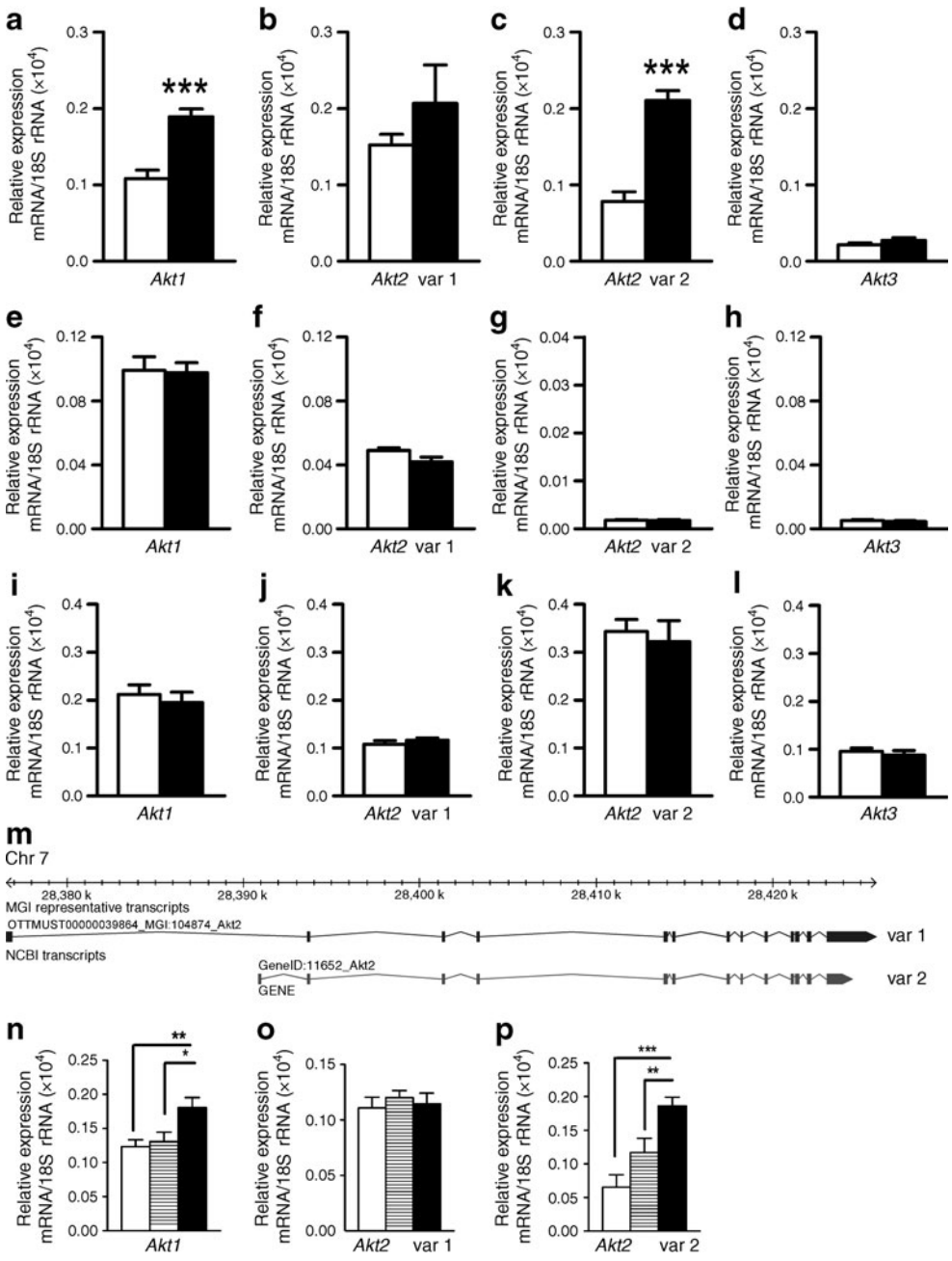

Fig. 3 Quantitative PCR of *Akt1*, *Akt2* (variant [var] 1 and var 2) and *Akt3* mRNA in (**a–d**) quadriceps muscle, (**e–h**) liver and (**i–l**) epididymal adipose tissue of male *sg/sg* mice (black columns) relative to wild-type littermates (white columns). n=7–8 per group, ***$p<0.001$ by t test. **m** Schematic representation of genomic structure of *Akt2* var 1 and *Akt2* var 2, and use of alternative promoter. Excerpt from MGI mouse genome browser at website as cited [45]. **n–p** Quantitative PCR of *Akt1, Akt2* var1 and *Ak2* var 2 mRNA in quadriceps muscle of male wild-type (white columns), heterozygous *sg/+* (striped columns) and homozygous *sg/sg* mice (black columns) (3–7 months old). n=10–12 per group, *$p<0.05$, **$p<0.01$ and ***$p<0.001$ by one-way ANOVA with Bonferroni's post hoc test. All bar graph values mean±SEM, with relative mRNA expression normalised against 18S rRNA

not variant 1) mRNA in quadriceps muscle in heterozygous mice was intermediate between wild-type and homozygous staggerer (*sg/sg*) mice (Fig. 3o, p). In contrast *Akt1* mRNA expression was similar to that of wild-type mice (Fig. 3n).

We also determined by western blot analysis whether changes in mRNA expression correlated with changes in the protein levels of total AKT (Fig. 4a) and phosphorylated (serine amino acid residue 473 [ser473]) AKT (Fig. 4b) in quadriceps muscle of wild-type and *sg/sg* mice in the basal (unstimulated) state. We observed a significant increase in total AKT protein (normalised against glyceraldehyde-3-phosphate dehydrogenase [GAPDH] protein) in the skeletal muscle from *sg/sg* mice relative to wild-type littermate pairs (Fig. 4a), corresponding with the mRNA expression data. In addition, levels of the active phosphorylated (ser473) AKT species was also significantly increased (normalised against GAPDH) (Fig. 4b) in the basal condition.

Aberrant expression in sg/sg mice of genes involved in regulation of glucose tolerance and metabolic disease The

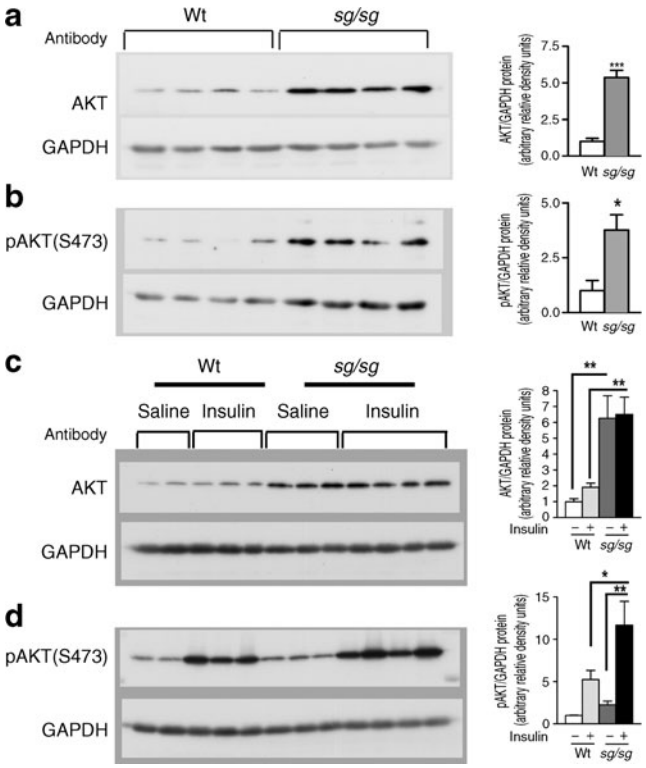

Fig. 4 Western blot analyses of (**a**) AKT and (**b**) pAKT relative to GAPDH in skeletal muscle (quadriceps) of male *sg/sg* and wild-type (WT) littermate control mice, with densitometry analysis of western blots; n=4 per group, mean±SEM; *p<0.05 and ***p<0.001 by t test. **c** Western blot analyses (representative blot from two experiments) of AKT and (**d**) pAKT relative to GAPDH in skeletal muscle (quadriceps) of male wild-type (Wt) and *sg/sg* littermate mice treated with saline and insulin (0.5 U/kg i.p. for 10 min). Densitometry was analysed using both experiments; n=4–6 per group, mean±SEM; *p< 0.05 and **p<0.01 two-way ANOVA with Bonferroni's post hoc test

nodes of the insulin signalling pathway (underscoring the central role of AKT2) are summarised in Fig. 5a. We used quantitative PCR to analyse mRNA expression of the *p85α* (also known as *Pik3r1*) and *p85β* (also known as *Pik3r2*) regulatory subunits of PI3K. However, no significant differences in expression were observed in the muscle of male *sg/sg* mice (Fig. 5b, c).

We also validated the differential expression of *Tbc1d1* (which encodes a Rab GTPase-activating protein, and the paralogue *Tbc1d4* [also known as *As160*]) and several other genes in the *sg/sg* mice (relative to wild-type littermates). These genes have been implicated in AKT signalling and the regulation of glucose tolerance and/or insulin sensitivity. For example, TBC1D1 has recently been identified (as an AKT substrate) in the insulin-stimulated AKT cascade that facilitates GLUT4 translocation [21] and regulates glucose uptake [22]. The *Tbc1d1* and *Tbc1d4* mRNA were significantly induced (about threefold) and decreased, respectively (Fig. 5d, e) in *sg/sg* mice. Serum- and glucocorticoid-inducible kinase 1 (*Sgk1*) was similarly induced by about threefold (Fig. 5f). Serum- and glucocorticoid-inducible kinase 1 modulates salt-dependent glucose uptake and mediates several PI3K responses, with emerging evidence suggesting it interacts with AKT kinases and mammalian transducer of regulated cAMP response element-binding protein 2 [23]. Polymorphisms (and increases) of paraoxonase 1 are associated with glucose intolerance and type 2 diabetes, and, consistent with the phenotype, was decreased by about twofold (Fig. 5g). Finally, *Tip47* (also known as *Plin3)* in skeletal muscle has been shown to maintain insulin sensitivity [24–26]; its mRNA was significantly induced by about 2.5-fold (Fig. 5h).

With regard to glucose transporters, we observed no changes in expression of *Glut1* (also known as *Slc2a1*) mRNA (data not shown); however, we did observe a small but significant increase in *Glut4* (also known as *Slc2a4*) mRNA expression (Fig. 5i). The increase in *Glut4* mRNA was reflected in a significant, approximately twofold increase in the level of GLUT4 protein after western blot analysis of *sg/sg* mice, relative to wild-type littermates (n=9; Fig. 5j).

The differential expression of these genes in muscle of *sg/sg* mice was consistent with improved insulin sensitivity, and with increased AKT levels and AKT phosphorylation. These analyses thus revealed that several components of the insulin signalling pathway are modulated in the *sg/sg* phenotype, these modulations being associated with decreased blood glucose and improved insulin signalling.

Staggerer mice display significantly elevated 'absolute levels' of pAKT and total AKT protein in the basal and insulin-stimulated states, and have enhanced ex vivo glucose uptake We subsequently examined whether *sg/sg* mice display increased insulin-mediated AKT phosphorylation. Whole-cell extracts from quadriceps muscles were

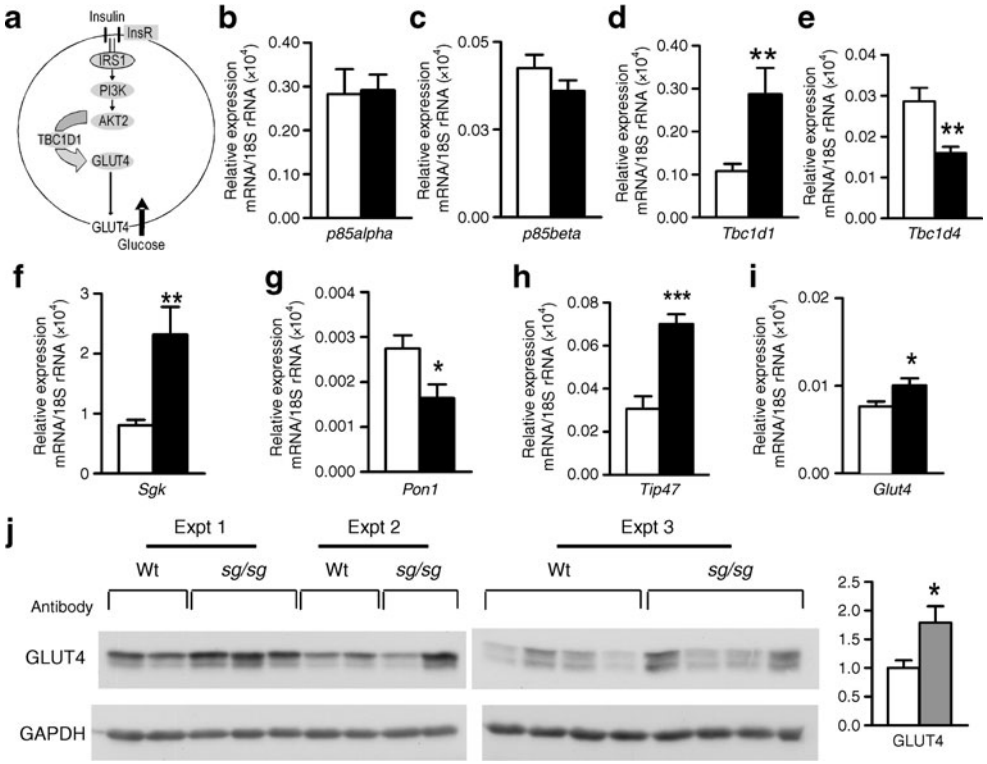

Fig. 5 **a** Schematic representation of the insulin-mediated glucose disposal pathway in skeletal muscle. InsR, insulin receptor. **b–i** Quantitative PCR of mRNA from skeletal muscle (quadriceps) of male *sg/sg* (black columns) mice relative to wild-type (Wt) littermates (white columns) for genes as labelled. Relative mRNA expression was normalised against 18S rRNA; n=7–8 per group, mean±SEM; *p<0.05, **p<0.01 and ***p<0.001, by t test. **j** Western blot analyses of GLUT4 in skeletal muscle (quadriceps) from male *sg/sg* and wild-type (WT) littermate control mice, with densitometry analysis (grey, *sg/sg*; white, wild-type littermate control) using both western blots; n=8–9 per group, mean±SEM; *p<0.05 by t test

isolated from saline- and insulin-injected mice were analysed by western blot analysis using antibodies specific to AKT and pAKT. We observed significantly elevated 'absolute levels' of total AKT protein (in the basal and insulin-stimulated states) in quadriceps muscle from *sg/sg* mice (normalised against GAPDH) (Fig. 4c). We also observed significantly elevated 'absolute levels' of insulin-stimulated phosphorylation of AKT (ser473) in *sg/sg* mice (normalised against GAPDH) (Fig. 4d).

We next investigated whether the improved insulin sensitivity and elevated 'absolute' levels of AKT and pAKT in *sg/sg* mice resulted in increased ex-vivo glucose uptake in EDL muscle (type II fast twitch glycolytic muscle) (Fig. 6). In keeping with the increase in AKT level and phosphorylation, EDL muscle of *sg/sg* mice showed significantly higher rates of 2-deoxy-D-glucose uptake than wild-type mice in the basal and insulin-stimulated state.

Discussion

A recent review [8] underscored the diverse roles of RORs in development, immunity, circadian rhythm, lipid homeostasis and metabolism. Moreover, (dysfunctional) levels of this NR are associated with ataxia, autoimmune disease, dyslipidaemia, atherosclerosis and resistance to diet-induced obesity. The *sg/sg* mice are *Rorα*-deficient, *sg/sg* is a non-functional null allele and *sg/sg* mice do not express functional RORα [12]. Moreover, *sg/sg* mice display identical phenotypes to the *Rorα*-knockout mice, which do not produce RORα protein [12, 27].

The pathophysiological phenotypes in *sg/sg* mice are consistent with changes in the expression of genes such as *Srebp-1c* (also known as *Srebf1*), *Apoa1*, *Apoc3* and *IκBα* (also known as *Nfkbia*) [4, 7, 9, 28]. We have previously shown that *sg/sg* mice have significantly reduced *Rorα1* and *Rorα4* expression [9], and display increased expression of Lipin 1 and *Pgc-1α* (also known as *Ppargc1a*), and

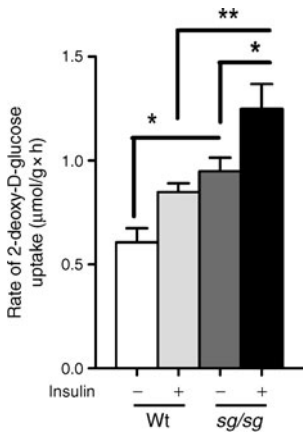

Fig. 6 2-Deoxy-D-[^{3}H]glucose uptake assays of control and insulin-treated EDL muscle explants from male wild-type (Wt) and *sg/sg* mice (3–7 months old); n=7–10 per group, mean±SEM; *p<0.05 and **p<0.01 By two-way ANOVA with Bonferroni's post hoc test

decreased expression of *Srebp-1c*. The differential expression of these genes is consistent with the ability of *sg/sg* mice to resist diet-induced obesity and hepatic triacylglycerol accumulation [9].

To date, the role of RORα in the control of insulin sensitivity and glucose uptake remains obscure. The links and interactions between fatty acid and carbohydrate homeostasis in whole-body physiology, and in the pathophysiological development of glucose intolerance and insulin resistance underscore the need to examine the role of this NR in carbohydrate metabolism. Consequently, we examined the outcomes of aberrant RORα function in muscle, a tissue that accounts for the bulk of insulin-stimulated glucose disposal [29]. The (male) *sg/sg* mice present with significantly reduced fasting serum glucose and improved insulin sensitivity relative to wild-type littermates. Our results differ from those of Kang et al. who showed a lack of serum glucose phenotype in *sg/sg* compared with their wild-type mice [30]. The nature of this difference is still not known. Recently it has been suggested that, in mice, a 6 h fast provides a more physiologically relevant baseline, increased sensitivity and fewer confounding variables for the evaluation of serum glucose and glucose tolerance [31, 32].

Expression profiling identified differential regulation of genes in the skeletal muscle of *sg/sg* mice. Similarly, bi-directional changes in gene expression have been observed in liver of *sg/sg* mice [30]. In the analysis reported here, the upregulated subset of genes was associated with cardiovascular and metabolic disease, cell death, infection, immunity and inflammation. This is consistent with the defined role of RORα in atherosclerosis, lipid homeostasis, fat deposition, obesity and inflammation [8, 33]. Interestingly, the primary signalling pathway upregulated in muscle was the PI3K–AKT pathway, a central control point for insulin-stimulated glucose uptake. Two RNA variants of *Akt2* have been identified. We showed that *Akt2* variant 2 was highly expressed in epididymal fat and (quadricep) skeletal muscle, but not in liver of wild-type mice. We observed significant differential expression of *Akt1* and *Akt2* variant 2 in quadriceps of *sg/sg* mice, indicating a specific role for these signalling molecules in skeletal muscle.

Interestingly, we had previously demonstrated that transgenic muscle-specific overexpression of dominant-negative RORα1 leads to decreased *Akt2* mRNA expression, glucose intolerance, decreased insulin-stimulated phosphorylation of AKT and glucose uptake [17]. In this study, we observed that decreased (and dysfunctional) expression of *Rorα* (*1* and *4*) led to increased *Akt2* mRNA expression and improved insulin sensitivity, and increased levels of basal and insulin-stimulated phosphorylation of AKT and of glucose uptake.

Notably in this context, the staggerer strain has a deletion of the fifth exon encoding the ligand binding domain. The resulting frame shift encodes 'non-sense RNA' and introduces a premature stop codon. However, further analysis by northern blot [34] and RT-PCR [9] revealed greater than tenfold decreases in *Rorα1* and *Rorα4* mRNA expression. Moreover, northern blot analysis [12] was not able to detect the transcript in homozygous *sg/sg* mice. Gold et al. [34] state that this is consistent with 'degradation of the mutant mRNA through the non-sense mediated decay pathway'. In agreement with this, *sg/sg* mice do not produce the RORα protein. Although initially thought to have a dominant-negative form of RORα, *sg/sg* mice are in fact *Rorα*-deficient. In contrast to this, our previous study [17] used a construct that abundantly/ectopically expresses a stable truncated *Rorα* mRNA transcript with an in-frame stop codon. The truncated *Rorα* ΔDE includes the encoded amino acids 1–235 [17], but lacks the ligand binding domain and part of the hinge region. McBroom et al. [35] and Lau et al. [2] reported that deletion of this segment preserved DNA recognition and binding, suppressed transactivation and operated in a dominant-negative manner. In addition, Hamilton et al. [11] reported that the staggerer mutation is located in a similar position and produces a non-functional ligand binding domain.

This apparent paradox in ROR function has a precedence in the NR field and there are a number of factors to consider. In the first instance, our previous transgenic mouse model overexpressed a dominant-negative *Rorα1* transcript, specifically in skeletal muscle [17]. In comparison, the present study investigated *sg/sg* mice, which lack *Rorα1* and *Rorα4* expression in all tissues. Second, in mice lacking NR, 'bona fide' target genes are often derepressed, resulting in paradoxically increased expression [36]. We suggest the data are consistent with decreased (and dysfunctional) RORα expression leading to derepression and increase of *Akt2* mRNA expression. This is consistent with our observation that RORα is selectively recruited to the *Akt2* promoter and that dominant-negative overexpression represses *Akt2* mRNA expression [17]. More importantly, these studies clearly identify a link between *Rorα* expression, *Akt2* and glucose tolerance.

Previous studies [37, 38] have demonstrated transcriptional regulation of *Rev-erbα* (also known as *Nr1d1*) by RORα and decreased *Rev-erbα* mRNA expression in *sg/sg* mice [37]. However, this did not explain the increased expression of *Akt2* mRNA in the *sg/sg* mice. For example, we also observe decreased expression of *Rev-erbα* in *sg/sg* mice; however, there was no decrease in REV-ERBα protein (ESM Fig. 6). This is consistent with another report [39], which showed 'dissociation between mRNA and protein levels'.

In the context of improved insulin sensitivity, glucose uptake and increased AKT levels, we also observed increased *Tbc1d1* and *Glut4* expression. This is entirely

consistent with Peck and colleagues [21], who very recently showed that activated AKT phosphorylates TBC1 domain family, member 1 (TBC1D1) and enhances glucose uptake. We also used quantitative PCR to validate the differential expression of several other mRNAs, including *Pon1* and *Sgk1*, that are associated with type 2 diabetes, insulin secretion and metabolic syndrome [40, 41] and also appeared in several categories, similarly to *Akt2*.

We were particularly interested in AKT2, as this protein is an integral component of the signalling pathway controlling insulin signalling. For example, several investigations have reported that AKT2 is a major regulator of insulin-mediated glucose disposal in skeletal muscle. Aberrant *Akt2* gene expression in rodents is associated with insulin resistance, type 2 diabetes-like syndrome, age-dependent lipodystrophy [42, 43] and phosphorylation of TBC1D1.

The threefold increase in expression of *Tbc1d1* mRNA, initially appears paradoxical. Mutations in *Tbc1d1* are associated with morbid obesity, for example, the R125W mutation in humans. However, the functional outcomes of these mutations have not yet been characterised. In the context of improved insulin sensitivity, glucose uptake and increased AKT level (and phosphorylation), we also observed increased *Tbc1d1* and *Glut4* expression. These observations are consistent with the latest studies on *Tbc1d1* function. Peck and colleagues recently demonstrated that AKT phosphorylation of TBC1D1 (similar to AKT substrate, 160 kDa/TBC1 domain family, member 4) enables GLUT4 translocation [21]. Second, the obesity-related mutant R125W *Tbc1d1* decreases insulin-stimulated glucose transport [22]. Both groups suggest that impaired glucose uptake provides a potential mechanism for the associated obesity. The differential (and increased) production of this Rab GTPase-activating protein, coupled to increased pAKT level in *sg/sg* mice, is interesting from the perspective of a potential contribution to resistance to diet-induced obesity in *sg/sg* mice via increased glucose uptake.

Interestingly, and consistent with increased insulin sensitivity, *sg/sg* mice showed enhanced insulin-mediated AKT phosphorylation and glucose uptake (and increased GLUT4 protein levels) in skeletal muscle. Recently, Duez et al. [44] showed that overexpression of *Rorα4* in 3T3-L1 cells inhibits pre-adipocyte differentiation, *Glut4* transcription and insulin-induced glucose uptake. In agreement with this, we have shown here that the GLUT4 protein level was increased in muscle from *sg/sg* mice.

In conclusion, the NR, RORα, is involved in regulation of AKT production and signalling, and glucose uptake. This study extends previous evidence that RORα performs a critical role in the regulation of adiposity. Further studies are required to examine whether this NR can be therapeutically exploited.

Acknowledgements G.E.O Muscat is a Principal Research Fellow and M.J. Watt a Senior Research Fellow of the National Health and Medical Research Council of Australia (NHMRC). This study was supported by project grants to G.E.O Muscat from the NHMRC and by Diabetes Australia Research Trust.

Duality of interest The authors declare that there is no duality of interest associated with this manuscript.

References

1. Schmitz-Peiffer C (2000) Signalling aspects of insulin resistance in skeletal muscle: mechanisms induced by lipid oversupply. Cell Signal 12:583–594
2. Lau P, Nixon SJ, Parton RG, Muscat GE (2004) RORalpha regulates the expression of genes involved in lipid homeostasis in skeletal muscle cells: caveolin-3 and CPT-1 are direct targets of ROR. J Biol Chem 279:36828–36840
3. Mamontova A, Seguret-Mace S, Esposito B et al (1998) Severe atherosclerosis and hypoalphalipoproteinemia in the staggerer mouse, a mutant of the nuclear receptor RORalpha. Circulation 98:2738–2743
4. Raspe E, Duez H, Gervois P et al (2001) Transcriptional regulation of apolipoprotein C-III gene expression by the orphan nuclear receptor RORalpha. J Biol Chem 276:2865–2871
5. Kumar N, Solt LA, Conkright JJ et al (2010) The benzenesulfoamide T0901317 [N-(2, 2, 2-trifluoroethyl)-N-[4-[2, 2, 2-trifluoro-1-hydroxy-1-(trifluoromethyl)ethyl]phenyl]-benzenesulfonamide] is a novel retinoic acid receptor-related orphan receptor-alpha/gamma inverse agonist. Mol Pharmacol 77:228–236
6. Raichur S, Lau P, Staels B, Muscat GE (2007) Retinoid-related orphan receptor gamma regulates several genes that control metabolism in skeletal muscle cells: links to modulation of reactive oxygen species production. J Mol Endocrinol 39:29–44
7. Vu-Dac N, Gervois P, Grotzinger T et al (1997) Transcriptional regulation of apolipoprotein A-I gene expression by the nuclear receptor RORalpha. J Biol Chem 272:22401–22404
8. Jetten AM (2009) Retinoid-related orphan receptors (RORs): critical roles in development, immunity, circadian rhythm, and cellular metabolism. Nucl Recept Signal 7:e003
9. Lau P, Fitzsimmons RL, Raichur S, Wang SC, Lechtken A, Muscat GE (2008) The orphan nuclear receptor, RORα, regulates gene expression that controls lipid metabolism: Staggerer (sg/sg) mice are resistant to diet-induced obesity. J Biol Chem 283:18411–18421
10. Matysiak-Scholze U, Nehls M (1997) The structural integrity of ROR alpha isoforms is mutated in staggerer mice: cerebellar coexpression of ROR alpha1 and ROR alpha4. Genomics 43:78–84
11. Hamilton BA, Frankel WN, Kerrebrock AW et al (1996) Disruption of the nuclear hormone receptor RORalpha in staggerer mice. Nature 379:736–739
12. Dussault I, Fawcett D, Matthyssen A, Bader JA, Giguere V (1998) Orphan nuclear receptor ROR alpha-deficient mice display the cerebellar defects of staggerer. Mech Dev 70:147–153
13. Smith AG, Muscat GE (2005) Skeletal muscle and nuclear hormone receptors: implications for cardiovascular and metabolic disease. Int J Biochem Cell Biol 37:2047–2063

14. Smith AG, Muscat GE (2006) Orphan nuclear receptors: therapeutic opportunities in skeletal muscle. Am J Physiol Cell Physiol 291:C203–C217
15. Muscat GE, Wagner BL, Hou J et al (2002) Regulation of cholesterol homeostasis and lipid metabolism in skeletal muscle by liver X receptors. J Biol Chem 277:40722–40728
16. Matthaei S, Stumvoll M, Kellerer M, Haring HU (2000) Pathophysiology and pharmacological treatment of insulin resistance. Endocr Rev 21:585–618
17. Raichur S, Fitzsimmons RL, Myers SA et al (2010) Identification and validation of the pathways and functions regulated by the orphan nuclear receptor, ROR alpha1, in skeletal muscle. Nucleic Acids Res 38:4296–4312
18. Brozinick JT Jr, Birnbaum MJ (1998) Insulin, but not contraction, activates Akt/PKB in isolated rat skeletal muscle. J Biol Chem 273:14679–14682
19. Watt MJ, Dzamko N, THomas WG et al (2006) CNTF reverses obesity-induced insulin resistance by activating skeletal muscle AMPK. Nat Med 12:541–548
20. Bertin R, Guastavino JM, Portet R (1990) Effects of cold acclimation on the energetic metabolism of the staggerer mutant mouse. Physiol Behav 47:377–380
21. Peck GR, Chavez JA, Roach WG et al (2009) Insulin-stimulated phosphorylation of the Rab GTPase-activating protein TBC1D1 regulates GLUT4 translocation. J Biol Chem 284:30016–30023
22. An D, Toyoda T, Taylor EB et al (2010) TBC1D1 regulates insulin- and contraction-induced glucose transport in mouse skeletal muscle. Diabetes 59:1358–1365
23. Lang F, Gorlach A, Vallon V (2009) Targeting SGK1 in diabetes. Expert Opin Ther Targets 13:1303–1311
24. Sztalryd C, Bell M, Lu X et al (2006) Functional compensation for adipose differentiation-related protein (ADFP) by Tip47 in an ADFP null embryonic cell line. J Biol Chem 281:34341–34348
25. Wolins NE, Quaynor BK, Skinner JR et al (2006) OXPAT/PAT-1 is a PPAR-induced lipid droplet protein that promotes fatty acid utilization. Diabetes 55:3418–3428
26. Bell M, Wang H, Chen H et al (2008) Consequences of lipid droplet coat protein downregulation in liver cells: abnormal lipid droplet metabolism and induction of insulin resistance. Diabetes 57:2037–2045
27. Steinmayr M, Andre E, Conquet F et al (1998) staggerer phenotype in retinoid-related orphan receptor alpha-deficient mice. Proc Natl Acad Sci USA 95:3960–3965
28. Delerive P, Monte D, Dubois G et al (2001) The orphan nuclear receptor ROR alpha is a negative regulator of the inflammatory response. EMBO Rep 2:42–48
29. Baron AD, Brechtel G, Wallace P, Edelman SV (1988) Rates and tissue sites of non-insulin- and insulin-mediated glucose uptake in humans. Am J Physiol 255:E769–E774
30. Kang HS, Angers M, Beak JY et al (2007) Gene expression profiling reveals a regulatory role for ROR alpha and ROR gamma in phase I and phase II metabolism. Physiol Genomics 31:281–294
31. Andrikopoulos S, Blair AR, Deluca N, Fam BC, Proietto J (2008) Evaluating the glucose tolerance test in mice. Am J Physiol Endocrinol Metab 295:E1323–E1332
32. McGuinness OP, Ayala JE, Laughlin MR, Wasserman DH (2009) NIH experiment in centralized mouse phenotyping: the Vanderbilt experience and recommendations for evaluating glucose homeostasis in the mouse. Am J Physiol Endocrinol Metab 297:E849–E855
33. Boukhtouche F, Mariani J, Tedgui A (2004) The "CholesteROR" protective pathway in the vascular system. Arterioscler Thromb Vasc Biol 24:637–643
34. Gold DA, Gent PM, Hamilton BA (2007) ROR alpha in genetic control of cerebellum development: 50 staggering years. Brain Res 1140:19–25
35. McBroom LD, Flock G, Giguere V (1995) The nonconserved hinge region and distinct amino-terminal domains of the ROR alpha orphan nuclear receptor isoforms are required for proper DNA bending and ROR alpha-DNA interactions. Mol Cell Biol 15:796–808
36. Wagner BL, Valledor AF, Shao G et al (2003) Promoter-specific roles for liver X receptor/corepressor complexes in the regulation of ABCA1 and SREBP1 gene expression. Mol Cell Biol 23:5780–5789
37. Delerive P, Chin WW, Suen CS (2002) Identification of Reverb (alpha) as a novel ROR(alpha) target gene. J Biol Chem 277:35013–35018
38. Raspe E, Mautino G, Duval C et al (2002) Transcriptional regulation of human Rev-erbalpha gene expression by the orphan nuclear receptor retinoic acid-related orphan receptor alpha. J Biol Chem 277:49275–49281
39. Wang J, Lazar MA (2008) Bifunctional role of Rev-erbalpha in adipocyte differentiation. Mol Cell Biol 28:2213–2220
40. Friedrich B, Weyrich P, Stancakova A et al (2008) Variance of the SGK1 gene is associated with insulin secretion in different European populations: results from the TUEF, EUGENE2, and METSIM studies. PLoS ONE 3:e3506
41. Schwab M, Lupescu A, Mota M et al (2008) Association of SGK1 gene polymorphisms with type 2 diabetes. Cell Physiol Biochem 21:151–160
42. Cho H, Mu J, Kim JK et al (2001) Insulin resistance and a diabetes mellitus-like syndrome in mice lacking the protein kinase Akt2 (PKB beta). Science 292:1728–1731
43. Garofalo RS, Orena SJ, Rafidi K et al (2003) Severe diabetes, age-dependent loss of adipose tissue, and mild growth deficiency in mice lacking Akt2/PKB beta. J Clin Invest 112:197–208
44. Duez H, Duhem C, Laitinen S et al (2009) Inhibition of adipocyte differentiation by RORalpha. FEBS Lett 583:2031–2036
45. Mouse Genome Informatics. MGI Mouse Genome Browser on build 37. Available from http://gbrowse.informatics.jax.org/cgi-bin/gbrowse/mouse_current/?start=28376571;stop=28425845;ref=7, accessed 20 January 2011